

<https://doi.org/10.1038/s44304-024-00002-1>

Flood teleconnections from levees undermine disaster resilience

Check for updates

Abolfazl Hojjat Ansari¹, Alfonso Mejia²✉ & Raj Cibin^{1,2}

Inland levees can amplify flood risk in unprotected communities by altering floodwater levels away from their location. While these nonlocal effects of levees, which we term flood teleconnections, have been studied for specific river segments, their impact on flood risks along a river network remains underexplored. By combining data-driven, hydrodynamic, and economic models, we quantify the magnitude, spatial distribution, and economic damages associated with flood teleconnections for a large river network system with extensive levees. We find that due to levees, the 100-year flood inundation extent grows by 25% of the total levee-protected area regionally, and the flood inundation depth increases by up to 2 m at specific locations. Levees also increase the vulnerability of unprotected, marginalized communities to flooding. Our results demonstrate that flood teleconnections are spatially widespread, involve unaccounted costs, and can lead to flood inequities. These findings will be critical to climate adaptation efforts in flood-prone regions.

Inland levees are used for flood protection globally^{1–4}. Although levees can protect against flooding locally by preventing floodwaters from entering the area behind them, they have negative unintended consequences^{5–8}. By constricting flood waves and reducing floodplain storage, levees increase flood water levels and velocities, negatively impacting unprotected communities away from their location^{6,9}. Using both empirical^{8,10} and modeling⁶ approaches, these negative impacts have been studied for specific levee systems and rivers, such as segments of the Mississippi River^{11–14}, but the impacts on diverse towns and cities along a river network remain underexplored. Despite the widespread adoption of levees in many parts of the world and their application in global climate adaptation models^{15–17}, there is a limited evidence base of the nonlocal influence of levees on flood damages and vulnerabilities at a system (basin) level.

Climate change is driving changes in flood patterns globally^{18–23}. Based on future climate projections, flood hazard is expected to increase in many regions of the world in the coming decades^{24–26}. In the United States, the severity and frequency of floods have increased over time at many locations²⁷ and are expected to continue to rise in the future^{28,29}. This implies that the current flood protection level of levees, such as setting the height of levees to withstand a 100-year flood, will be insufficient in the future, and existing levees will need to be enlarged to maintain present protection levels in the future. This flood risk management challenge is compounded by levees that are past or approaching the end of their design life. In the United States, of the levees listed in the National Levee Database approximately 85%

are designated as nonaccredited³⁰, highlighting that a significant number of levees need to be upgraded even just to meet today's accreditation standards.

To be effective in supporting flood resilience and climate adaptation, infrastructure investments need to account for levees' negative externalities^{31,32}, like regional flood teleconnections. We use the concept of flood teleconnection to refer to the shift or transfer of flood risk away from a levee, which occurs when changes in floodwater levels and velocities caused by the presence of a levee propagate through the river network to impact nearby and distal communities^{7,10}. Although hydraulic theory can explain a levee's nonlocal effect on flood inundation along a river segment, this effect is substantially more challenging to untangle at broad spatial scales, where interactions between multiple levees, floodplain development, and the river network morphology can amplify flood risk in nontrivial ways. Moreover, by not recognizing flood teleconnections explicitly, previous large-scale flood inundation studies may have overestimated the benefits of levees^{15,25,33,34}. Here, we model and quantify the magnitude, spatial distribution, and economic damages associated with flood teleconnections along the river network of the Susquehanna River Basin (SRB)—the main tributary to the largest estuary in North America, the Chesapeake Bay. There are more than 140 major levee systems in the SRB (Fig. 1A and Fig. S1), totaling over 180 miles of protected floodplain and safeguarding numerous towns and cities against catastrophic flood damages and losses.

¹Department of Agricultural and Biological Engineering, The Pennsylvania State University, University Park, PA, USA. ²Department of Civil and Environmental Engineering, The Pennsylvania State University, University Park, PA, USA. ✉e-mail: aim127@psu.edu

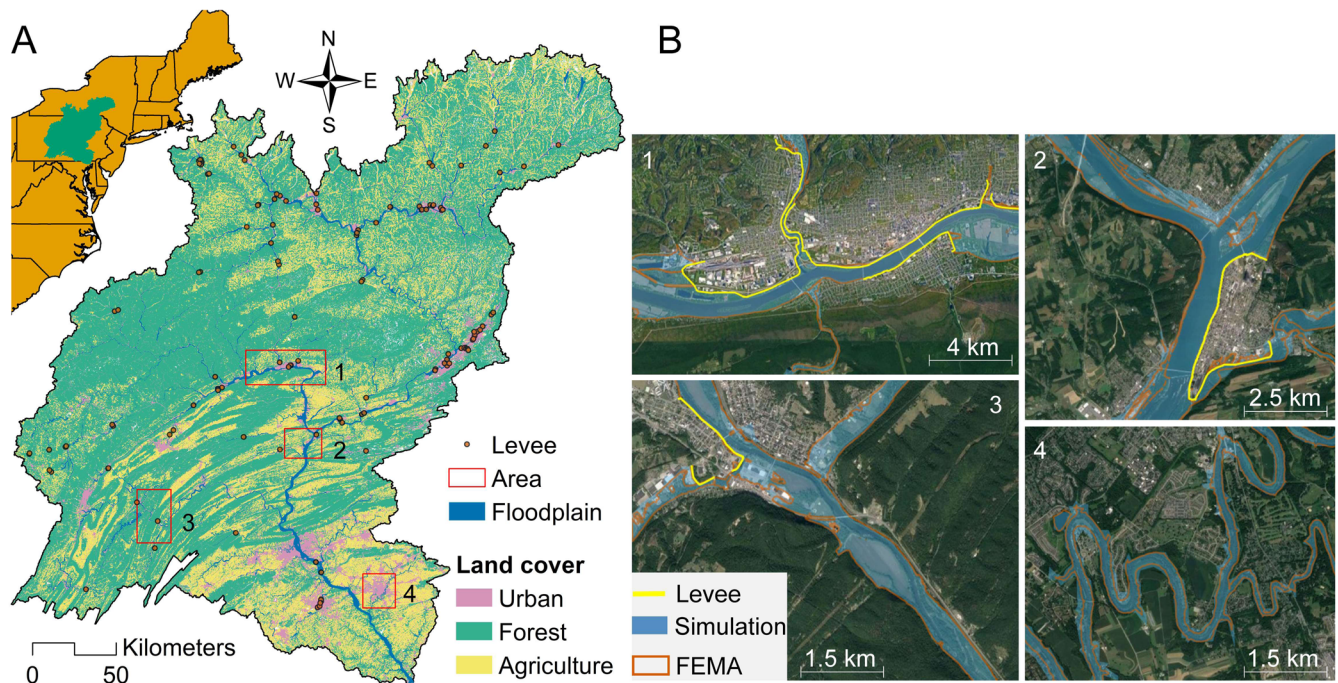


Fig. 1 | Susquehanna River Basin (SRB) and comparison of flood inundation maps. **A** Map illustrating the spatial distribution of land cover, location of levees, 100-year flood inundation extent along the river network, and areas (labeled 1 through 4 and indicated with red boxes) used to evaluate the flood

inundation simulations in the SRB. The inset map shows the location of the SRB in the U.S. Northeast. **B** Visual comparison between the simulated flood inundation extents and FEMA 100-year flood hazard maps for the areas labeled 1 through 4 in **A**.

Results

Flood inundation simulations for a large river network with extensive levees

To simulate the flood inundation associated with different extreme flood events, we combined statistical³⁵ and 1D/2D hydrodynamic models of extreme flood³⁶ (Materials and Methods). The statistical model was used to determine extreme flood events of different return periods (5, 10, 50, 100, and 500 years), which were used as boundary conditions in the hydrodynamic model. The hydrodynamic model was used to simulate flood inundation for scenarios representing different combinations of return periods and flood protection (with and without levees). For the statistical model, we used a regionalization approach (Materials and Methods), together with the generalized extreme value distribution, to improve the estimation of extreme flood events.

Using daily streamflow observations for 118 gauged sites in the SRB (Fig. S2), the regionalized statistical model augments local information at a target location by pooling data from other regional sites with similar hydrological characteristics to the target location (Supplementary Methods). For example, at one gauged site with only 10 years of daily streamflow data (Fig. S2), the uncertainty was reduced by as much as 70% for the 100-year flood compared to a nonregionalized version of the statistical model (Fig. S3). Similar reductions in uncertainty were observed at other sites with short records. Our methodology represents a substantial improvement over that of previous flood inundation studies that have not considered the uncertainty associated with the estimation of extreme flood events.

For the 100-year flood event, the flood inundation extents simulated using our hydrodynamic model compare well against the Federal Emergency Management Agency (FEMA) flood inundation maps (Fig. 1B), which are widely used for flood plain management and to inform flood insurance decisions. To compare the flood inundation maps, we used a fitness statistic to measure the degree of agreement or overlap between FEMA's flood inundation extent and the simulated inundation predicted by independent, locally isolated models (areas 1 through 4 in Fig. 1A) that account for the presence of levees (Supplementary Methods). Based on these case studies (areas 1 through 4 in Fig. 1A and Table S1), we found that the

overlap was high—greater than 85% (Fig. S4A), indicating that our modeling results were consistent with FEMA flood inundation maps. In areas of flat terrain, like the deltaic subregion of the lower SRB, the overlap was lower—approximately 75% (Fig. S4A)—because the flood inundation simulation became more sensitive to the terrain resolution. This was further evaluated by testing the sensitivity of the hydrodynamic model to the terrain resolution. We also performed a comparison of the 100-year water levels between FEMA and the model outputs at different locations (Fig. S5). This comparison check showed that our model can reasonably simulate water levels, supporting the robustness of our inundation predictions.

The resolution of our regional flood inundation model for the SRB was 30 m. Comparing this model's results against simulations with 3- and 10-m resolutions, we found that the performance of the regional model was comparable to that of the higher-resolution models (Fig. S4B). That is, the overlap between the regional and 3-m resolution models was comparable to the overlap between the 10- and 3-m models for various case studies, with values of the fitness statistic greater than 80% (Fig. S4B). For flood inundation depth, the maximum root mean square difference between the 30- and 3-m simulations was approximately 1 m, which is comparable to the minimum freeboard required by FEMA for levee certification³⁷, suggesting that our simulation error was within FEMA's safety factor. However, in the deltaic subregion of the lower SRB, where flood teleconnections are negligible, we found that a finer resolution markedly improves flood inundation modeling (Fig. S6).

Flood teleconnections from levees across the river network

To model and quantify flood teleconnections, we simulated flood inundation with and without levees for different return periods. By comparing these two flood protection scenarios against each other for a given return period, we distinguished between protected floodplain areas (PFAs) and teleconnected floodplain areas (TFAs). The PFA is the area behind a levee that is safeguarded from flooding by being disconnected from the floodplain. TFAs are flood inundation areas that are indirectly modified by the presence of levees, including impacted areas that are nearby or far away from the levees. TFAs result from increases in the extent or depth of floodwaters

due to levees. We measured TFAs using both the total flood inundation area affected by the change in flood inundation extent and that affected by the change in depth due to levees for a given return period, which yielded two different estimates of TFAs. For the change in the flood inundation area based on depth, we used a minimum threshold of 0.3 m to focus on TFAs that can result in costly flood damages.

Our results show that the total TFA accounts for roughly 0.8% (equivalent to 26% of the total PFA) and 9.0% of the 100-year flood inundation area, based on the change in inundation extent and depth, respectively, in the SRB (Table S2). The large difference in the size of TFAs based on the change in inundation depth versus inundation extent indicates that increases in floodwater levels due to levees are mostly confined to narrow floodplains.

We found that TFAs can occur over long distances, negatively impacting communities that are farther away from a levee than would be anticipated from examining a levee's neighboring areas alone (Fig. 2A). Previous studies have often focused on areas in the vicinity of levees, potentially missing these long-distance interactions. Here, these flood teleconnections tend to emerge from the interactions between multiple levees and the river morphology. For instance, our results show that several upstream levees in series drive flood inundation increases at a distant teleconnection site 32 km downstream from the levees (Fig. 2A, B), with floodwater levels increasing by 1.3 m just downstream of the levees (Fig. 2C)

and by 0.6 m at the long-distance teleconnection site (Fig. 2D). These elevation changes are substantiated by recent FEMA observations, which recorded flood elevation increases for a 100-year flood event ranging between 0.3 and 1.8 meters in the vicinity and downstream areas of these levees³⁸.

In our long-distance teleconnection example (Fig. 2), flood amplification occurred because the negative effect of levees on flood inundation was enhanced by the river morphology. The floodplain is narrower and the banks steeper upstream, where the levees are located (Fig. 2C), than at the distant teleconnection site (Fig. 2D), which facilitates the propagation of floodwaters and thus the transfer of flood risk downstream. Moreover, the increase in flood inundation depth at the distant teleconnection site was equivalent to 40% of the increase expected from a 500-year flood (Fig. 2D). That is, at this teleconnection site, the 100-year flood level approached the value of a 500-year event due to the flood amplification caused by levees. Overall, across the SRB, the increases in flood inundation depth were as large as 2 m in floodplain areas and communities unprotected by levees.

To assess the stability of the simulated TFAs, we evaluated their sensitivity to the uncertainty in the boundary condition, since this is a major source of modeling error³⁵. For a subregion in the eastern SRB with a high concentration of levees (area 5 in Fig. S2), we estimated the 95% confidence intervals of the 100-year flood events used as the boundary condition in the hydrodynamic model (Material and Methods). Using the lower and upper

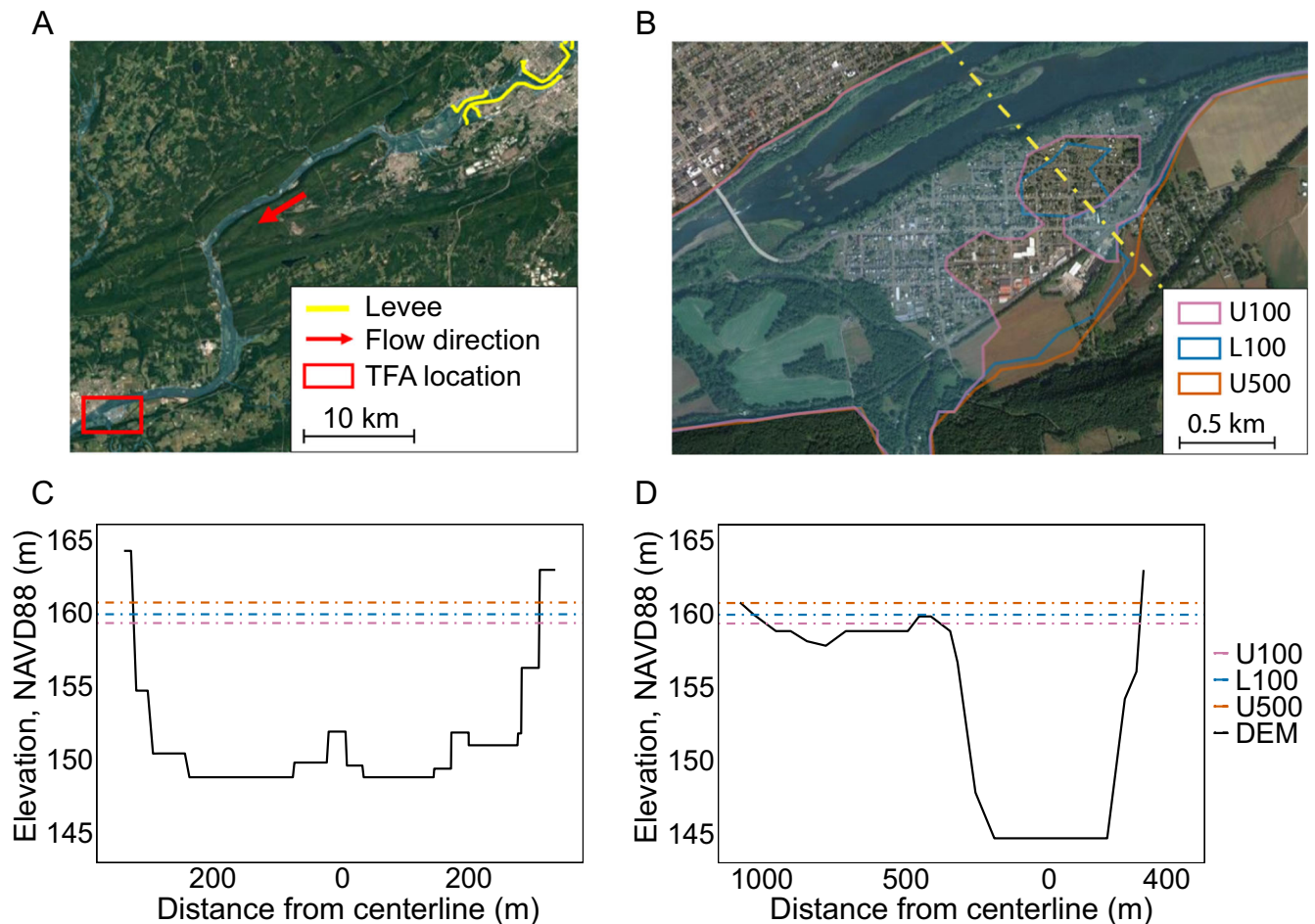


Fig. 2 | Illustration of long-distance flood teleconnection. **A** Map depicting the location of levees (yellow lines) and a distant flood teleconnection site (red box), approximately 32 km downstream from the levees. This panel highlights the spatial extent of levee influence on flood inundation. **B** Mapping comparison of 100-year flood inundation levels with (blue line; L100) and without (purple line; U100) levees at the distant flood teleconnection site (red box in panel A), demonstrating how levees can alter flood dynamics far downstream. **C** Comparison of floodwater levels

at a floodplain cross-section just downstream of the levees in **A**. **D** Comparison of floodwater levels at a floodplain cross-section (yellow dashed line in **B**) on the distant teleconnection site (red box in **A**). Notably, in both **C**, **D**, the 100 year flood level with levees (L100) closely approaches the magnitude of a 500-year flood without levees (U500), emphasizing the impact of levees on flood risk propagation downstream. These flood levels are shown alongside the cross-section elevations from the digital elevation model (DEM), illustrating the shift in floodwater behavior due to levees.

bounds of these confidence intervals as two distinct sets of boundary conditions, the uncertainty of the flood estimates was propagated through the hydrodynamic model, which allowed us to obtain a lower and upper estimate of TFA. Based on the change in the 100-year flood inundation extent, the total TFA ranged from 9.2 to 13.8 km², which is equivalent to 28% and 33%, respectively, of the total PFA (Table S3). It also shows that our regional estimate of the TFA—26% of the total PFA—was not unduly influenced by the uncertainty of extreme flood events, given that this estimate is relatively close to our uncertainty range of 28% to 33%.

We also tested the sensitivity of TFAs to the terrain resolution. Our regional estimate of TFA was based on 30-m flood inundation simulations. Comparing these 30-m simulations against 10-m ones for our selected subregion in the SRB (area 5 in Fig. S2), our results showed that even though the total PFA and TFA decreased slightly in terms of the change in flood inundation extent (Table S4), the ratio between the TFA and PFA remained approximately similar at 25% for both the 30 and 10-m simulations. For the flood inundation depth, the change in TFA due to terrain resolution fell mostly within the TFA ranges obtained from considering the uncertainty in the boundary condition. For example, the TFA range was 20% to 23.5% of the total 100-year flood inundation area for the 30-m simulation due to the uncertainty in the boundary condition (Table S3), while for the 10-m simulation, the TFA was equal to 21.5% (Table S4). This indicates that TFA is more influenced by the uncertainty in the boundary condition than the terrain resolution, highlighting the importance of our regionalization approach for quantifying and reducing the uncertainty of extreme flood events.

Cost-benefit and vulnerability analyses of the basinwide flood teleconnections

To further assess the impact of TFAs on flood risk, we performed a cost-benefit analysis (Materials and Methods). For flood events of different return periods, we estimated the economic benefit as the avoided flood damages to structures in PFAs and calculated the cost as the flood damages associated with TFAs. This cost is typically unaccounted for in flood inundation studies. By accounting for the immediate cost (not considering the levees’ lifespan) associated with TFAs, we found that it increased with the return period across the SRB from \$54 million for a 5-year flood to \$380 million for a 500-year flood (Fig. 3A). These costs represent 15% and 27% of the benefit from levees, respectively. Therefore, the cost associated with TFAs may be substantial, underscoring the need to include flood teleconnection costs when planning to upgrade levees.

Taking into consideration the design lives, capital, and maintenance costs of levees, we found that TFAs contribute about 14% of the total expected annual cost, whereas capital and maintenance costs account for 57% and 29%, respectively, for a 100-year flood (Fig. 3B). For a 500-year

flood, the contribution of TFAs to the total cost is about 9% (Fig. 3B). However, the cost associated with flood teleconnections reduces the benefit-cost ratio by as much as 14% regionally. The benefit-cost ratio decreases from 1.35 to 1.16 and from 0.83 to 0.75 for 100-year and 500-year floods (Fig. 3B), respectively, due to flood teleconnections. These benefit-cost ratios of 0.75 and 1.16 that are near or below one—and below the recommended target of 2.5 for federal flood projects in the United States³⁹—emphasize the critical need to quantify and assess TFAs in future levee planning. Similarly, low benefit-cost ratios were reported by Bradt and Aldy³⁹ for large levee projects in the United States.

TFAs affect communities that are already highly vulnerable to flooding. These are communities that require attention to ensure that flood mitigation outcomes are equitable and just. We found that the flood teleconnections associated with levee-protected, higher-income communities could negatively impact unprotected, lower-income communities (Fig. 4A). For example, households in census block group B1 are levee protected and have a higher income, on average, than households in block groups B2 and B3 (Fig. 4A, B), which are affected by TFAs. The households in block group B3 are below the poverty line in Pennsylvania (Fig. 4B). This represents a type of flood inequity in which flood risk is transferred from a levee-protected area to an unprotected one with greater flood vulnerability.

To assess the influence of TFAs on flood vulnerability (Materials and Methods), we divided all the block groups impacted by TFAs into four vulnerability quadrants—high, medium-high, medium-low, and low vulnerability – on the basis of their per capita income and race (percent Black or African American population) (Fig. 4C). Given that TFAs can occur over long distances, exposure to TFAs affects heterogeneous communities across the SRB (Fig. 4C), independently of their vulnerability. The population distribution among block groups in the quadrants with high, medium-high, medium-low, and low vulnerability was 9.5%, 31.4%, 1.6%, and 57.5%, respectively, of the total population affected by TFAs (Table S5), indicating that in terms of the number of impacted individuals, low vulnerability areas are the most exposed to TFAs, whereas medium-low vulnerability areas are the least exposed. However, for block groups with a Black or African American population greater than 12% (the statewide percentage in Pennsylvania), we found that the majority of the population – 85% of them (Table S5) – fall into the high-vulnerability quadrant (Fig. 4C), indicating inequality in the distribution of TFAs. This suggests that historically marginalized communities are more likely to experience TFAs while also having less capacity to cope with flooding.

Discussion

By modeling flood inundation in a regional river network with a high concentration of levees, we found that flood teleconnections are spatially widespread and can span longer distances than generally recognized. They

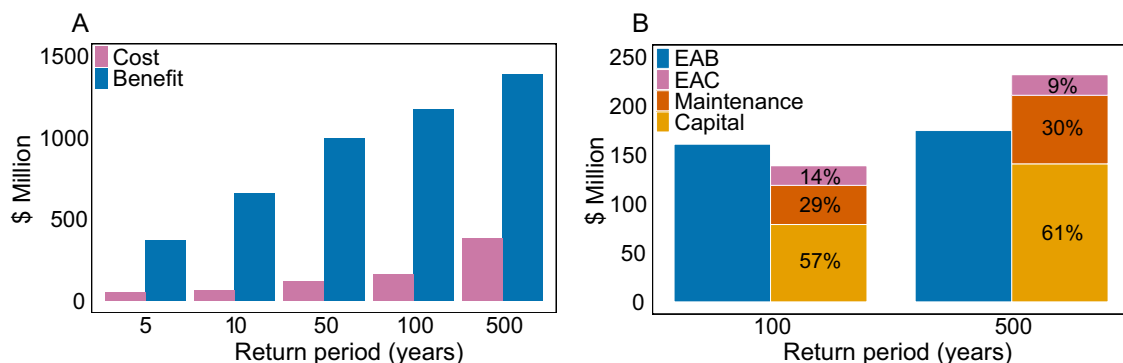


Fig. 3 | Cost-benefit analysis of levees considering flood teleconnections. **A** Total immediate (not considering the levees’ lifespan) cost and benefit of levees for specific flood return periods (5, 10, 50, 100, and 500 years), illustrating the economic impact for each scenario. **B** Expected annual cost (EAC) and expected annual benefit (EAB) over a 50-year lifespan of levees for 100- and 500-year flood protection scenarios.

This panel highlights that 14% and 9% of the total cost of levees for 100-year and 500-year flood scenarios, respectively, stem from teleconnection effects. The analysis incorporates U.S. standard capital and maintenance costs, with adjustments for additional height requirements and no discount on capital costs over time.

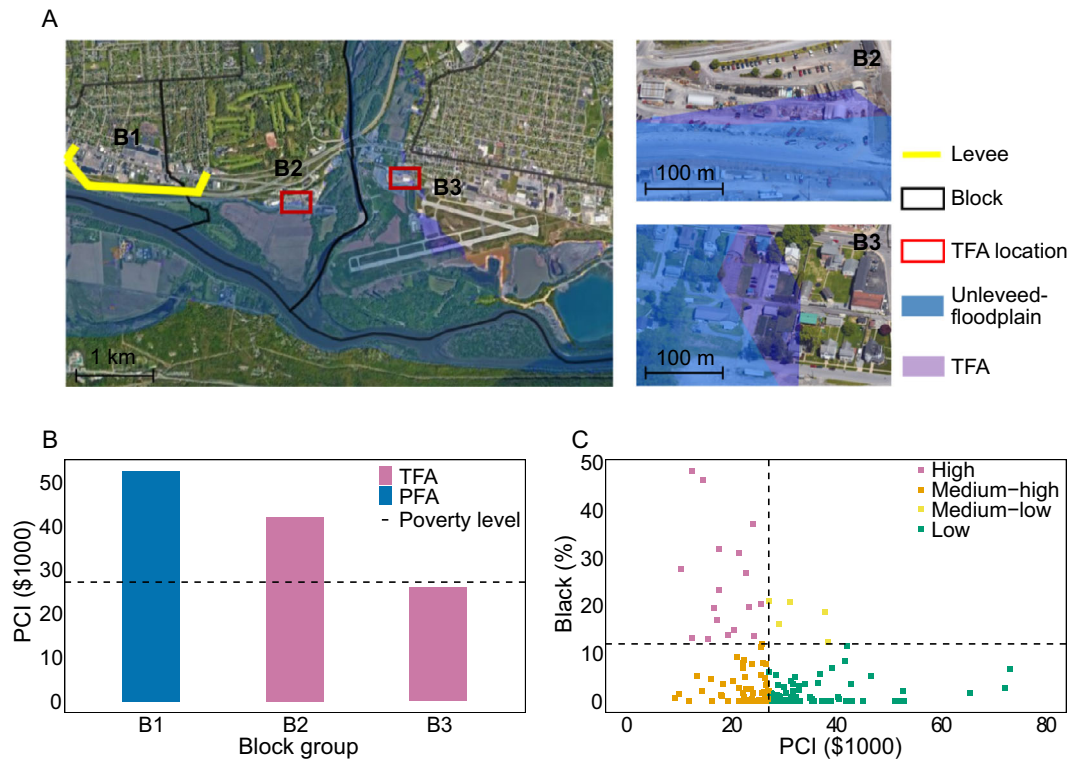


Fig. 4 | Exposure and social vulnerability to flood teleconnections. **A** Map illustrating the 100-year flood inundation extent for three neighboring census block groups—B1, B2, and B3. The map focuses on three census block groups for clarity, but the analysis was performed for all the census block groups in the SRB. The red boxes indicate the areas shown in the inset flood maps (right), which highlight the flood teleconnection for block groups B2 and B3 using the 100-year flood inundation extent with (purple shading) and without (blue shading) levees. **B** Plot of the per capita income (PCI) for the same block groups, B1, B2, and B3, in **A** (only three block groups are shown for clarity, but the analysis was done for all block groups in the

SRB). The dashed line represents the poverty level in Pennsylvania. **C** Plot of all the block groups in the SRB impacted by 100-year flood teleconnections as a function of each group’s percentage of Black or African American population and per capita income. That is, each dot in the plot represents a different census block group in the SRB. The plot is divided into four quadrants based on a 12% Black or African American population and \$27,185 per capita income, which are the statewide percentage of Black or African American population and the poverty level, respectively, in Pennsylvania. The quadrants are used to categorize the block groups into high, medium-high, medium-low, and low flood vulnerability.

can also result in flood inequities when they affect underserved populations that are vulnerable to flooding. Given the prevalence of levees, this type of flood inequity is relevant to communities in river basins other than the SRB³⁹. We also found that the flood damages associated with flood teleconnections may be substantial, ranging across return periods from approximately 9% to 27% of the damage averted by levees. These results have implications for flood resilience and climate adaptation efforts across flood-prone communities.

Flood teleconnections from levees can diminish flood disaster resilience. Our results show that the magnitude and spatial extent of flood teleconnections increase with the return period. This means that enlarging current levees or building new ones to offset increases in future flood hazards will amplify the flood risk in unprotected communities. This flood risk amplification can weaken disaster resilience since it implies that as more levees are built in a region, the overall flood protection benefits from levees and the region’s capacity to cope with extreme flooding would progressively decline over time. This reduction in regional disaster resilience may manifest in different ways. For instance, if unprotected communities affected by flood teleconnections lack flood insurance, this will delay recovery after a flood event and thus hamper disaster resilience.

Failing to account for flood teleconnections could result in flood risk misattribution and overestimation of the climate adaptation benefits of levees. For example, if levees were enlarged to protect against the current 500-year flood—a standard being considered for climate adaptation purposes by the U.S. government⁴⁰—rather than the 100-year flood, the cost of flood teleconnections would increase by more than 2-fold in the SRB based on our results. If flood teleconnections were omitted from the analysis,

however, this cost would likely be misattributed to climate change through the change in the flood standard. To support regional disaster resilience and climate adaptation, it is thus critical for levee engineering design to integrate preventive measures against flood teleconnections. For instance, consideration should be given to design factors that can minimize and mitigate flood teleconnections—such as the location, size, number, and spacing of levees—within a regional setting.

Flood inundation maps, like FEMA’s 100-year flood hazard maps and similar products⁴¹, fail to identify and depict flood teleconnections, even though flood maps are an essential and widely used tool for analyzing, managing, and communicating flood risk. For instance, nonaccredited levees—levees that do not meet the criteria to provide protection against a 100-year flood—are often excluded from the flood inundation modeling and mapping processes. Although this exclusion has the advantage of capturing the residual risk (the risk associated with a levee failure)^{1,6}, it also leads to the underestimation of flood teleconnections, which may result in the misrepresentation of the flood hazard for certain communities. Using flood inundation maps to communicate the ability of flood teleconnections to generate flood risk may foster flood resiliency—for example, by improving flood literacy and flood related decisions made by individuals and communities, such as purchasing flood insurance, flood-proofing, or advocating for a particular flood measure⁴².

As in any model-based study, our approach has limitations. We used steady-state dynamics to simulate flood inundation. For a particular extreme storm, the magnitude and range of regional flood teleconnections will depend on the storm characteristics (duration, intensity, and spatiotemporal variability) and on unsteady flood wave dynamics, which might lead to flood

teleconnection estimates that differ from the steady-state ones. Nonetheless, our approach is consistent with the modeling and mapping processes used to generate large-scale^{25,33,34} and regulatory⁴³ flood inundation maps, implying that flood teleconnections would be a prevalent feature of those maps if they were to map or identify them. Additionally, we ignored the residual risk from levees. This mainly affected our cost-benefit calculations, suggesting that the benefit from levees is even less than that estimated here.

Historically, extensive levee construction has been preceded by record-breaking flooding in the SRB, peaking with Hurricane Agnes in 1972^{44,45}. The large-scale flooding associated with Agnes prompted the addition of approximately 60 miles of levees, which account for a large proportion of the flood teleconnections in our analysis. Thus, unless different strategies are proactively pursued and planned, the next unprecedented flood is likely to trigger further levee construction, compounding the flood risk amplification caused by levees. Nature-based solutions that restore the natural storage capacity of altered terrestrial ecosystems like floodplains, wetlands, and forests are being pursued as a sustainable alternative to levees and flood protection infrastructure^{46,47}. However, their efficient design and implementation require identifying flood risk transfers along the river network and delineating the connection between upstream interventions (such as restoring wetlands) and downstream flood risk reductions in individual floodplain communities, making our flood teleconnection construct relevant beyond levees.

Methods

The Susquehanna River Basin

The Susquehanna River is the longest river on the East Coast of the United States (Fig. S1), draining an area of approximately 71,000 km², including half of the land area of the Commonwealth of Pennsylvania and portions of the states of New York and Maryland. The majority of the land cover in the SRB is made up of forestlands (65% of the SRB area), followed by pastures/croplands (22%) and urban areas (8%)⁴⁸.

The SRB, with a population of 4,200,000⁴⁹, is one of the most flood-prone regions in the United States, experiencing devastating floods on average every 14 years and over \$150 million in flood damages annually⁵⁰. Flooding is frequently caused by the remnants of Atlantic hurricanes, mesoscale convective storms, and/or rapid snow melts and snowfalls followed by heavy rains. Flood hazard mitigation is aided by over 180 miles of levees along the Susquehanna River network³⁰ (Fig. S1).

To focus our assessment of model performance and conduct different model sensitivity analyses, we selected four flood-prone areas in the SRB (labeled 1 through 4 in Fig. S2 and Table S1). These four flood-prone areas have experienced more than five significant flood events since 1950, each exceeding a return period greater than 10 years. Flooding in these areas is mitigated by levees mostly designed to withstand a 100-year flood event. In addition, to assess the effect of extreme flood event uncertainty on flood teleconnections, we selected a larger subregion with a high concentration of levees in the eastern SRB (labeled 5 in Fig. S2).

Data

Using the U.S. Geological Survey (USGS) watershed boundary dataset⁵¹, we delineated the SRB's catchment boundaries and stream network at the 12-digit hydrological unit code (HUC-12) level. At this level, the SRB is comprised of 911 catchments with an average area of 78.1 km², ranging from 1.6 to 187.2 km². The topography was represented using digital elevation model (DEM) data from the USGS National Elevation Dataset (NED)⁵¹. The NED provides elevation data with a consistent resolution, coordinate system, elevation unit, and horizontal and vertical datums⁵². For modeling flood inundation, we used DEM data at 3, 10, and 30-m resolutions. Land cover was characterized using the 2019 USGS National Land Cover Data (NLCD)⁵³ at a 30-m resolution. The SRB is intensively monitored through a network of USGS streamflow gauges (Fig. S2)⁵⁴. For the estimation of extreme flood events, we used daily streamflow data from gauges with at least 10 years of records⁵⁵. A total of 173 gauges were considered, covering the entire SRB; 25 of the gauges have records longer than 100 years.

Information about levees was obtained from the U.S. Army Corps of Engineers (USACE) National Levee Database (NLD)³⁰. In the SRB, over 200,000 residents and 70,000 building units with a total value of \$30 billion are protected by nearly 140 levees (Fig. 1A and S1), of which 80 (47 miles) are classified as nonaccredited³⁰, since they cannot provide protection against a 100-year flood event; 37 (90 miles) are designated as accredited; and the remaining is provisionally accredited. The average age of the levees is approximately 60 years (Fig. S1).

For the estimation of flood damage, we used the CoreLogic ParcelPoint database⁵⁶. This database contains the characteristics of U.S. properties and their sale transactions, with over 99% national coverage. Based on the characteristics of each property (land code, number of stories, and type of foundation) extracted from the CoreLogic database, flood damage functions were obtained from the FEMA Hazus database⁵⁷.

We also used socioeconomic and demographic data (population, income, and race) from the U.S. Census at the block group level⁵⁸. The data used were for 5-year averages in 2017–2021. To define the distribution of residents within each block group, we used the U.S. Environmental Protection Agency (EPA) dasymetric map at a 30-m resolution⁵⁹. This map redistributes the 2010 U.S. population from the census block level to a 30-m grid according to the land cover and slope. We updated the EPA map using the 5-year averages of the population values in 2017–2021.

Statistical model of extreme flood events

We used a regionalization approach, together with the generalized extreme value (GEV) distribution, to improve the estimation of extreme flood events at both gauged sites with short records (fewer than 30 years of records) and ungauged sites^{35,60}. We refer to this statistical model as the regional GEV (RGEV). The RGEV was applied at the HUC-12 level to estimate extreme flood events with different return periods—5-, 10-, 50-, 100-, and 500-year flood events with 20%, 10%, 2%, 1%, and 0.2% annual chances of occurrence, respectively. These flood estimates were used as boundary conditions in the hydrodynamic model to simulate flood inundation along the SRB's river network. The mathematical details of the RGEV model are presented in the Supplementary Methods.

To account for the uncertainty of flood estimates from the RGEV model, nonparametric stratified bootstrapping was used to resample the streamflow records. Stratified bootstrapping ensures that records in dry and wet periods are included and that the bootstrapped samples are representative of the climate history. To preserve the spatial dependence among gauges in the bootstrapped samples, records were randomly drawn from four strata (four 30-year periods, from 1900 to the end of 2021) with equal probability and from the same years for all gauges. Figure S6 illustrates one of the bootstrapped samples. Using the RGEV model and the stratified bootstrapping approach, we estimated flood event magnitudes with 95% confidence bands. This is illustrated for USGS gauge 01502632 (Fig. S3), located in the Upper Susquehanna at Bainbridge, New York (Fig. S2).

Configuration of the hydrodynamic flood inundation model

To model and map the flood inundation depth and extent, we used the LISFLOOD-FP 1D/2D hydrodynamic model³⁶. This state-of-the-art model has been used for large-scale simulations of flood inundation in a variety of contexts^{29,61–64}. We ran the model using different DEM resolutions (3, 10, and 30 m), with a sub-grid-scale representation of stream channels⁵⁵ at the HUC-12 catchment level. To estimate the channel geometry, we used bankfull channel dimensions from regional hydraulic-geometry scaling relationships⁶⁶. This approach is reasonable when channel bathymetry data are not available^{67,68}. The hydraulic-geometry relationships accounted for the difference in channel dimensions between streams underlain by carbonate and noncarbonate rocks⁶⁶. Using the DEM “burning” approach as well as data (crest level and geometric attributes) from the NLD³⁰, levees were incorporated into the hydrodynamic model^{29,69}. For smaller streams narrower than the DEM resolution, levee positions were adjusted by one grid cell backward. Consequently, we restricted the floodplain by elevating DEMs at the levee locations. The channel roughness values were assumed to

be constant and equal to 0.045^{70,71}, whereas the floodplain values varied based on the 2019 NLCD land cover types⁵³.

Validation of flood inundation simulations

To validate the regional hydrodynamic model for the SRB, we compared our flood inundation results against flood inundation maps from FEMA. FEMA provides floodplain inundation maps for 100- and 500-year floods. FEMA's 100-year flood inundation map is the reference map for the National Flood Insurance Program (NFIP) and flood emergency measures nationwide. To make this comparison more meaningful, we used FEMA's 100-year peak flows as the boundary condition in LISFLOOD FP, rather than using the flood estimates from our statistical RGEV model (Fig. S4A). We used a fitness statistic to quantify the degree of agreement between the modeled and FEMA flood maps. This statistic is provided in the Supplementary Methods.

Sensitivity analyses

We performed three different sensitivity analyses to check the robustness of our modeling results. First, we evaluated the sensitivity of the hydrodynamic model outputs – flood inundation extent and depth—to the terrain resolution. Second, by focusing on a subregion of the SRB with a high concentration of levees (area 5 in Fig. S2), we evaluated the effect of flood event uncertainty on flood teleconnections. Third, we evaluated the sensitivity of flood teleconnections to the terrain resolution. The modeling details associated with the sensitivity analyses are presented in the Supplementary Methods.

Flood damage estimation

For the two flood protection scenarios (with and without levees), we estimated the flood damages associated with different return periods (5, 10, 50, 100, and 500 years) across the SRB. For the 500-year flood event, we assumed that the levees' crest is high enough to prevent overtopping. This assumption represents a climate adaptation scenario in which levees are enlarged and reinforced to meet a 500-year protection level. In the SRB, 100-year floods are anticipated to increase in the future and lie somewhere in between the current 100-year and 500-year flood levels⁷¹. Thus, we considered the current 500-year flood as the protection level for levees against future 100-year flood events in the year 2100⁷¹. The current 500-year flood is also being considered as one of several national-level options for adapting infrastructure to future climate change in the United States⁴⁰.

For flood damage estimation, we used property sale transactions from the CoreLogic database⁵⁶ and depth-damage functions from FEMA's Hazus database⁵⁷. The Hazus database contains over 1200 depth-damage functions for different residential, commercial, and industrial properties⁵⁷. Thus, we accounted for flood damages to any structure in the flood inundation zone but not for damages to transportation systems, utilities, crops, or ecosystems. We assigned each type of building within our flood inundation delineations to a depth damage function based on the building code and structural properties (e.g., number of stories and type of foundation). If multiple depth-damage functions were available for a specific type of building, we estimated the percentage of damage by averaging over all the functions. We adjusted the sale amounts using annual Consumer Price Index (CPI) values from the U.S. Bureau of Labor Statistics⁷² for the sale date and 2020. For the two flood protection scenarios (with and without levees) and different return periods, we estimated the 2020-dollar value of flood damages across the SRB. The benefit of levees was estimated as the avoided flood damage in PFAs. The cost of levees was estimated as the flood damage associated with TFAs (Fig. S8).

To estimate the expected annual benefit and cost of levees, our analysis spanned a range of flood return periods from 5 to 500 years. We used typical values for United States levee capital and maintenance costs, assuming \$8 million per kilometer of length and per meter of height for capital costs, with maintenance costs at 1% of the capital cost^{15,33}. A zero-discount rate was applied for distributing the capital cost over the levees' standard 50-year lifespan. Levee height was determined by the difference between the levee

crest and ground elevation. For the 100-year protection level, our model assumes complete levee failure in the event of floods exceeding this threshold, based on the likelihood of 100% failure in such extreme conditions, thus rendering them non-protective. As a result, in these scenarios, both the projected benefits of protection and the associated unintended teleconnection costs are considered negligible. The same premise applies to the 500-year protection level, where we include protection up to the designed level but assume levee failure for more severe floods. Additional height requirements and corresponding capital and maintenance costs were recalculated for the 500-year scenario. The benefit-cost ratios were estimated as the ratio of the expected annual benefit to the expected annual cost, reflecting the long-term economic efficiency and impact of levees, balancing construction and maintenance costs against the benefits of flood damage prevention and the cost implications of flood teleconnections.

Flood vulnerability analysis

To assess the flood vulnerability, we determined the average percentage of the Black or African American population and the per capita income of individuals impacted by TFAs at the census block group level. Using the ratio of the Black or African American population and the poverty level in Pennsylvania, which are 12%⁷³ and \$27,180⁷⁴, respectively, we categorized block groups into four vulnerability quadrants: high (block groups with more than 12% Black or African American population and income below the poverty line), medium-high (block groups with less than 12% Black or African American population but per capita income below the poverty line), medium-low (block groups with more than 12% Black or African American population but with per capita income above the poverty line), and low (block groups with less than 12% Black or African American population and with per capita income above the poverty line) (Fig. S9 and Table S5). The number of people living in TFAs was estimated by the intersection of flood inundation and the updated dasymetric population density map from the EPA (Fig. S9). We assumed that the Black or African American population and the per capita income of individuals were uniformly distributed in each block group. Thus, in our vulnerability analysis, flood inequities resulted from the transfer of flood risk from levee-protected block groups to unprotected ones that had a relatively high Black or African American population and/or low-income households.

Data availability

The authors will make all the data, except for the proprietary CoreLogic data, and code available through a public data and code repository, such as HydroShare or GitHub.

Received: 5 October 2023; Accepted: 19 January 2024;

Published online: 28 February 2024

References

1. Montz, B. E. & Tobin, G. A. Livin' large with levees: lessons learned and lost. *Nat. Hazards Rev.* **9**, 150–157 (2008).
2. Burton, C. & Cutter, S. L. Levee failures and social vulnerability in the Sacramento-San Joaquin Delta area, California. *Nat. Hazards Rev.* **9**, 136–149 (2008).
3. Serra-Llobet, A., Tourment, R., Montané, A. & Buffin-Belanger, T. Managing residual flood risk behind levees: comparing USA, France, and Quebec (Canada). *J. Flood Risk Manag.* **15**, e12785 (2022).
4. Wenger, C. Better use and management of levees: reducing flood risk in a changing climate. *Environ. Rev.* **23**, 240–255 (2015).
5. Pinter, N., Ickes, B. S., Wlosinski, J. H. & Van der Ploeg, R. R. Trends in flood stages: contrasting results from the Mississippi and Rhine River systems. *J. Hydrol.* **331**, 554–566 (2006).
6. Pinter, N., Huthoff, F., Dierauer, J., Remo, J. W. & Dampitz, A. Modeling residual flood risk behind levees, Upper Mississippi River, USA. *Environ. Policy* **58**, 131–140 (2016).
7. Tobin, G. A. The levee love affair: a stormy relationship? *J. Am. Water Resour. Assoc.* **31**, 359–367 (1995).

8. Criss, R. E. & Shock, E. L. Flood enhancement through flood control. *Geology* **29**, 875–878 (2001).
9. Knox, R. L., Morrison, R. R. & Wohl, E. E. A river ran through it: floodplains as America's newest relict landform. *Sci. Adv.* **8**, eabo1082 (2022).
10. Heine, R. A. & Pinter, N. Levee effects upon flood levels: an empirical assessment. *Hydrol. Process.* **26**, 3225–3240 (2012).
11. Pinter, N., Jemberie, A. A., Remo, J. W. F., Heine, R. A. & Ickes, B. S. Flood trends and river engineering on the Mississippi River system. *Geophys. Res. Lett.* **35**, L23404 (2008).
12. Munoz, S. E. et al. Climatic control of Mississippi River flood hazard amplified by river engineering. *Nature* **556**, 95–98 (2018).
13. Criss, R. E. & Luo, M. Increasing risk and uncertainty of flooding in the Mississippi River basin. *Hydrol. Process.* **31**, 1283–1292 (2017).
14. Pinter, N., Thomas, R., Wlosinski, J. H. Regional impacts of levee construction and channelization, Middle Mississippi River, USA. In *Flood issues in contemporary water management*, Vol. 71 (eds Marsalek, J., Watt, W. E., Zeman, E. & Sieker, F.) NATO Science Series, 351–361 (Springer, Dordrecht, 2000).
15. de Ruig, L. T. et al. How the USA can benefit from risk-based premiums combined with flood protection. *Nat. Clim. Chang.* **12**, 995–998 (2022).
16. Davlasheridze, M., Fisher-Vanden, K. & Klaiber, H. A. The effects of adaptation measures on hurricane induced property losses: which FEMA investments have the highest returns? *J. Environ. Econ. Manag.* **81**, 93–114 (2017).
17. Dottori, F., Mentaschi, L., Bianchi, A., Alfieri, L. & Feyen, L. Cost-effective adaptation strategies to rising river flood risk in Europe. *Nat. Clim. Chang.* **13**, 196–202 (2023).
18. Gudmundsson, L. et al. Globally observed trends in mean and extreme river flow attributed to climate change. *Science* **371**, 1159–1162 (2021).
19. Markonis, Y., Papalexiou, S., Martinkova, M. & Hanel, M. Assessment of water cycle intensification over land using a multisource global gridded precipitation dataset. *J. Geophys. Res. Atmosph.* **124**, 11175–11187 (2019).
20. Blöschl, G. et al. Changing climate shifts timing of European floods. *Science* **357**, 588–590 (2017).
21. Winsemius, H. C. et al. Global drivers of future river flood risk. *Nat. Clim. Change* **6**, 381–385 (2016).
22. Milly, P. C. D., Wetherald, R. T., Dunne, K. & Delworth, T. L. Increasing risk of great floods in a changing climate. *Nature* **415**, 514–517 (2002).
23. Arnell, N. W. & Gosling, S. N. The impacts of climate change on river flood risk at the global scale. *Clim. Change* **134**, 387–401 (2016).
24. Merz, B. et al. Causes, impacts and patterns of disastrous river floods. *Nat. Rev. Earth Environ.* **2**, 592–609 (2021).
25. Willner, S. N., Levermann, A., Zhao, F. & Frieler, K. Adaptation required to preserve future high-end river flood risk at present levels. *Sci. Adv.* **4**, eaao1914 (2018).
26. Hirabayashi, Y. et al. Global flood risk under climate change. *Nat. Clim. Change* **3**, 816–821 (2013).
27. Ghanbari, M., Arabi, M., Kao, S. C., Obeysekera, J. & Sweet, W. Climate change and changes in compound coastal-riverine flooding hazard along the US coasts. *Earth's Future* **9**, e2021EF002055 (2021).
28. Marsooli, R., Lin, N., Emanuel, K. & Feng, K. Climate change exacerbates hurricane flood hazards along US Atlantic and Gulf Coasts in spatially varying patterns. *Nat. Commun.* **10**, 3785 (2019).
29. Bates, P. D. et al. Combined modeling of US fluvial, pluvial, and coastal flood hazard under current and future climates. *Water Resources Res.* **57**, e2020WR028673 (2021).
30. NLD, National Levee Database (<https://levees.sec.usace.army.mil/#/>) (2022).
31. Pinter, N. One step forward, two steps back on US floodplains (2005).
32. Hutton, N. S., Tobin, G. A. & Montz, B. E. The levee effect revisited: Processes and policies enabling development in Yuba County, California. *J. Flood Risk Manag.* **12**, e12469 (2019).
33. Ward, P. J. et al. A global framework for future costs and benefits of river-flood protection in urban areas. *Nat. Clim. Change* **7**, 642–646 (2017).
34. Tanoue, M., Taguchi, R., Alifu, H. & Hirabayashi, Y. Residual flood damage under intensive adaptation. *Nat. Clim. Change* **11**, 823–826 (2021).
35. Asadi, P., Engelke, S. & Davison, A. C. Optimal regionalization of extreme value distributions for flood estimation. *J. Hydrol.* **556**, 182–193 (2018).
36. Bates, P., Trigg, M., Neal, J., Dabrowa, A. UM LISFLOOD-FP, University of Bristol: Bristol (2013).
37. FEMA, Meeting the criteria for accrediting levee systems on flood insurance rate maps: How to guide for floodplain managers and engineers (https://www.fema.gov/sites/default/files/documents/fema_meeting-criteria-accrediting.pdf) (2021).
38. FEMA, Susquehanna River Flood Study Update (https://www.fema.gov/sites/default/files/2020-10/fema_susquehanna-river-flood-study_update_fact-sheet.pdf) (2020).
39. Bradt, J. T., Aldy, J. E. Private Benefits from Public Investment in Climate Adaptation and Resilience (2022).
40. Baecher, G. B. & Galloway, G. E. US Flood risk management in changing times. *Water Policy* **23**, 202–215 (2021).
41. FEMA, Federal Emergency Management Agency (FEMA) flood map (<https://www.fema.gov/flood-maps>) (2022).
42. Song, L., Michels, P., Shaw, A. The inequality of America's levee system (<https://www.motherjones.com/environment/2018/08/the-inequality-of-americas-levee-systems/>) (2022).
43. FEMA, Guidance for flood risk analysis and mapping floodplain boundary standards (FBS) (https://www.fema.gov/sites/default/files/2020-02/FBS_Guidance_Nov_2019.pdf) (2019).
44. Feuerstein, J. Hurricane Agnes and the Susquehanna: how devastation inspired mitigation (<https://www.washingtonpost.com/climate-environment/2022/06/19/hurricane-agnes-susquehanna-50years-storm/>) (2022).
45. Silver Jackets. Mitigation in the wake of Hurricane Agnes (<https://storymaps.arcgis.com/stories/646f43dcd46543858890e486473464b3>) (2022).
46. Opperman, J. J. & Galloway, G. E. Nature-based solutions for managing rising flood risk and delivering multiple benefits. *One Earth* **5**, 461–465 (2022).
47. Knox, R. L., Wohl, E. E. & Morrison, R. R. Levees don't protect, they disconnect: a critical review of how artificial levees impact floodplain functions. *Sci. Total Environ.* **837**, 155773 (2022).
48. SRBC, NASS CDL program (<https://nassgeodata.gmu.edu/CropScape/>) (2022).
49. SRBC, Susquehanna River Basin map (<https://www.srbc.net/portals/susquehanna-atlas/data-and-maps/susquehanna-basin/>) (2022).
50. SRBC, Susquehanna River Basin facts (<https://srbc.gov/our-work/fact-sheets/docs/river-basin-facts.pdf>) (2016).
51. USGS, The National Elevation Dataset (<https://apps.nationalmap.gov/downloader/>) (2023).
52. Gesch, D. et al. The national elevation dataset. *Photogrammetric engineering and remote sensing* **68**, 5–32 (2002).
53. NLCD, The National land cover dataset (<https://www.mrlc.gov/data?f%5B0%5D=category%3Aland%20cover&f%5B1%5D=region%3Aconus&f%5B2%5D=year%3A2019>) (2019).
54. USGS, Streamflow monitoring (<https://www.usgs.gov/programs/groundwater-and-streamflow-information-program/streamflow-monitoring>) (2023).
55. Roland, M. A., Stuckey, M. H. Development of regression equations for the estimation of flood flows at ungaged streams in Pennsylvania, (US Geological Survey), Technical report (2019).

56. CoreLogic, Property dataset (<https://www.corelogic.com/>) (2021).
57. FEMA, Hazus user & technical manuals (<https://www.fema.gov/flood-maps/tools-resources/flood-map-products/hazus/user-technical-manuals>) (2022).
58. Manson, S. M., Schroeder, J., Van Riper, D., Kugler, T., Ruggles, S. National Historical Geographic Information System, version 17.0 [dataset] (<https://www.ipums.org/>) (2022).
59. EPA, EnviroAtlas (<https://www.epa.gov/enviroatlas>) (2022).
60. Dupuis, D. J., Engelke, S. & Trapin, L. Modeling panels of extremes. *Ann. Appl. Stat.* **17**, 498–517 (2023).
61. Cantoni, E. et al. Hydrological performance of the ERA5 reanalysis for flood modeling in Tunisia with the LISFLOOD and GR4J models. *J. Hydrol. Reg. Stud.* **42**, 101169 (2022).
62. Fereshtehpour, M. & Karamouz, M. DEM resolution effects on coastal flood vulnerability assessment: deterministic and probabilistic approach. *Water Resour. Res.* **54**, 4965–4982 (2018).
63. Wilson, M. et al. Modeling large-scale inundation of Amazonian seasonally flooded wetlands. *Geophys. Res. Lett.* **34**, L15404 (2007).
64. Rajib, A., Liu, Z., Merwade, V., Tavakoly, A. A. & Follum, M. L. Towards a large-scale locally relevant flood inundation modeling framework using SWAT and LISFLOOD-FP. *J. Hydrol.* **581**, 124406 (2020).
65. Neal, J., Schumann, G. & Bates, P. A subgrid channel model for simulating river hydraulics and floodplain inundation over large and data sparse areas. *Water Resour. Res.* **48**, W11506 (2012).
66. Clune, J., Chaplin, J. & White, K. Comparison of regression relations of bankfull discharge and channel geometry for the glaciated and nonglaciated settings of Pennsylvania and Southern New York and StreamStats regional Curves Tool for Pennsylvania (2018).
67. Mejia, A. & Reed, S. Evaluating the effects of parameterized cross-section shapes and simplified routing with a coupled distributed hydrologic and hydraulic model. *J. Hydrol.* **409**, 512–524 (2011).
68. Mejia, A. I. & Reed, S. Role of channel and floodplain cross-section geometry in the basin response. *Water Resour. Res.* **47**, W09518 (2011).
69. Wing, O. E. et al. Estimates of present and future flood risk in the conterminous United States. *Environ. Res. Lett.* **13**, 034023 (2018).
70. Newlin, J. T. & Hayes, B. R. Hydraulic modeling of glacial dam-break floods on the West Branch of the Susquehanna River, Pennsylvania. *Earth Space Sci.* **2**, 229–243 (2015).
71. Sharma, S., Gomez, M., Keller, K., Nicholas, R. E. & Mejia, A. Regional flood risk projections under climate change. *J. Hydrometeorol.* **22**, 2259–2274 (2021).
72. CPI, CPI Home: U.S. Bureau of Labor Statistics (<https://www.bls.gov/cpi/>) (2022).
73. Census, The U. S. Census Bureau QuickFacts: Pennsylvania (<https://www.census.gov/quickfacts/fact/table/PA/PST045221>) (2021).
74. DCED, Pennsylvania Department of Community and Economic Development: Income eligibility (<https://dced.pa.gov/housing-and-development/weatherization/income-eligibility/>) (2022).

Acknowledgements

National Oceanic and Atmospheric Administration Pennsylvania Sea Grant 149483 and National Science Foundation Award 2332169.

Author contributions

All authors contributed to the conceptualization, methodology, investigation, and writing of the manuscript. AHA generated the results and figures. AM and RC were responsible for project supervision.

Competing interests

The authors declare no competing interests.

Additional information

Supplementary information The online version contains supplementary material available at <https://doi.org/10.1038/s44304-024-00002-1>.

Correspondence and requests for materials should be addressed to Alfonso Mejia.

Reprints and permissions information is available at <http://www.nature.com/reprints>

Publisher's note Springer Nature remains neutral with regard to jurisdictional claims in published maps and institutional affiliations.

Open Access This article is licensed under a Creative Commons Attribution 4.0 International License, which permits use, sharing, adaptation, distribution and reproduction in any medium or format, as long as you give appropriate credit to the original author(s) and the source, provide a link to the Creative Commons licence, and indicate if changes were made. The images or other third party material in this article are included in the article's Creative Commons licence, unless indicated otherwise in a credit line to the material. If material is not included in the article's Creative Commons licence and your intended use is not permitted by statutory regulation or exceeds the permitted use, you will need to obtain permission directly from the copyright holder. To view a copy of this licence, visit <http://creativecommons.org/licenses/by/4.0/>.

© The Author(s) 2024